



Durham Research Online

Deposited in DRO:

08 March 2011

Version of attached file:

Published Version

Peer-review status of attached file:

Peer-reviewed

Citation for published item:

Kaliteevski, M.A. and Brand, S. and Garvie-Cook, J. and Abram, R.A. and Chamberlain, J.M. (2008) 'Terahertz filter based on refractive properties of metallic photonic crystal.', *Optics express.*, 16 (10). pp. 7330-7335.

Further information on publisher's website:

<http://dx.doi.org/10.1364/OE.16.007330>

Publisher's copyright statement:

2008 The Optical Society. This paper was published in *Optics Express* and is made available as an electronic reprint with the permission of OSA. The paper can be found at the following URL on the OSA website: <http://www.opticsinfobase.org/abstract.cfm?URI=oe-16-10-7330> Systematic or multiple reproduction or distribution to multiple locations via electronic or other means is prohibited and is subject to penalties under law.

Additional information:

Use policy

The full-text may be used and/or reproduced, and given to third parties in any format or medium, without prior permission or charge, for personal research or study, educational, or not-for-profit purposes provided that:

- a full bibliographic reference is made to the original source
- a [link](#) is made to the metadata record in DRO
- the full-text is not changed in any way

The full-text must not be sold in any format or medium without the formal permission of the copyright holders.

Please consult the [full DRO policy](#) for further details.

Terahertz filter based on refractive properties of metallic photonic crystal

M. A. Kaliteevski, S. Brand*, J. Garvie-Cook, R. A. Abram, and J. M. Chamberlain

Department of Physics, Durham University, South Road, Durham DH1 3LE, United Kingdom

Corresponding author: stuart.brand@dur.ac.uk

Abstract: We propose a new type of pass-band filter, in this case designed to operate in the terahertz frequency regime, possessing two separate pass-bands utilizing the distinction between positive and negative refraction in a photonic crystal prism. The prism is formed from a two-dimensional hexagonal arrangement of metallic rods. In order to understand the operation of the filter we both consider the photonic bandstructure of the associated infinite photonic structure and carry out simulations of the refraction properties of the prism using finite-difference time-domain software.

©2008 Optical Society of America

OCIS codes: Photonic crystals(160.5298), Electromagnetic optics (260.2110).

References and links

1. V. G. Veselago, "The electrodynamics of substances with simultaneously negative values of ϵ and μ ," Sov. Phys. Usp. **10**, 509-514 (1968).
 2. C. Luo, S. G. Johnson, J. D. Joannopoulos, and J. B. Pendry, "All-angle negative refraction without negative effective index," Phys. Rev. **B65**, 201104(R) (2002).
 3. E. Ozbay, I. Bulu, K. Guven, H. Caglayan, and K. Aydin, "Observation of negative refraction and focusing in two-dimensional photonic crystals," Jpn. J. Appl. Phys. **45**, 6064-6070 (2006).
 4. S-T Wu, M. S. Li, and Y-G Fuh, "Unusual refractions in photonic crystals based on polymer-dispersed liquid crystal films," Appl. Phys. Letts. **91**, 251117 (2007).
 5. D. Wang, L. Ran, H. Chen, M. Mu, J. A. Kong and B-I. Wu, "Active left-handed material collaborated with microwave varactors," Appl. Phys. Letts. **91**, 164101 (2007).
 6. S. Brand, R. A. Abram and M. A. Kaliteevski, "Complex photonic band structure and effective plasma frequency of a two-dimensional array of metal rods," Phys. Rev. **B75**, 035102 (2007).
 7. A. J. Gallant, M. A. Kaliteevski, S. Brand, D. Wood, M. Petty, R. A. Abram and J. M. Chamberlain, "Terahertz frequency passband filters," J. Appl. Phys. **102**, 023102 (2007).
 8. A. J. Gallant, M. A. Kaliteevski, D. Wood, M., C. Petty, R. A. Abram, S. Brand, G. P. Swift, D. A. Zeze and J. M. Chamberlain, "Passband filters for terahertz radiation based on dual metallic photonic structures," Appl. Phys. Letts **91**, 161115 (2007).
 9. FDTD simulations were carried out using the Omnisim[®] software package.
-

1. Introduction

Some time ago Veselago [1] observed that in a uniform material characterised by both negative permittivity and permeability the Poynting vector of an electromagnetic (EM) wave in the medium is antiparallel to its wavevector, giving rise to interesting effects such as negative refraction. More recently, the realisation of such effects has been investigated by employing non-uniform metamaterial structures. Although much work has been centred upon attempts to achieve negative permittivity and permeability simultaneously, this is not in fact a necessary condition to observe negative refraction in photonic structures. Indeed, Luo, *et al.*, [2] demonstrated theoretically that negative refraction could be achieved via the lowest photonic band of a dielectric structure possessing neither a negative refractive index nor a negative group velocity for EM waves. Others such as Ozbay, *et al.*, [3] have succeeded in the experimental observation of negative refraction in the microwave regime. Hence, negative refraction is a well established concept and the focus is now increasingly on the utilization rather than the demonstration of the effect. For example Wu, *et al.*, [4] have employed a polymer-dispersed liquid crystal photonic structure to obtain angle-dependent switching in the visible region, and Wang, *et al.*, [5] have demonstrated beam steering using a prism formed

from microwave frequency resonators/varactors. In recent work we have theoretically and experimentally demonstrated the use of photonic structures consisting of finite two-dimensional (2-D) square arrays of metallic pillars to achieve filtering of radiation in the terahertz frequency regime [6, 7]. The initial work was extended, to achieve a narrowing of the pass-band by using a dual array structure involving two arrays of the same period but different pillar diameters [8]. Only normal incidence was considered in that work. Here we theoretically demonstrate another approach which considers oblique incidence and utilizes the distinction between positive and negative refraction in a prism-like 2-D hexagonal metallic pillar array structure to achieve the THz filter properties. In this case the properties of the filter naturally depend on the parameters of the structure, but are also in principle tunable to some extent by varying the angle of incidence.

2. Results and discussion

Figure 1 shows the dispersion relation with the electric field, E , polarised parallel to the pillars in a hexagonal metallic photonic crystal (PC) with lattice constant $a = 200 \mu\text{m}$ formed by gold pillars with diameter $d = 80 \mu\text{m}$. The results were obtained using a hexagonal structure version of the complex bandstructure calculations described elsewhere [6]. With E parallel to

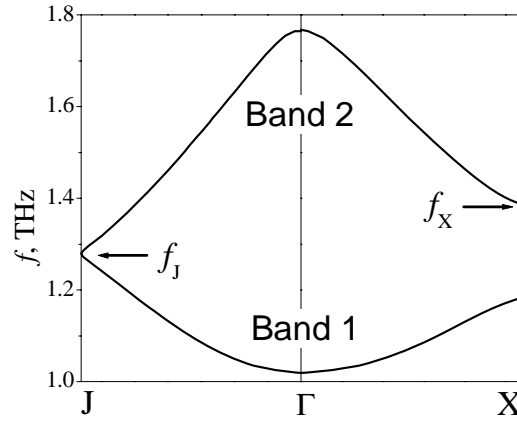


Fig. 1. The dispersion relation for an E -polarized electromagnetic wave in the hexagonal photonic crystal.

the pillars, there is an effective plasma frequency (~ 1.0 THz in this case) below which an EM wave cannot propagate. In PCs at low frequency, the shape of the 2-D equifrequency surface (EFS) is nearly circular, but in general, the bands are more complicated. It is significant that for this system the light-line lies entirely outside the region shown and therefore all photonic bands are in principle accessible to experimental investigation. For example, at the J point the frequency in the photonic crystal is $f_J = 1.28$ THz whereas the corresponding frequency in the vacuum is 1 THz.

The group velocity of the Bloch wave is defined as $v_g = \nabla_k \omega$ and for the symmetry directions $\Gamma - X$ and $\Gamma - J$ this is along the same axis as the wavevector, and we have that the group velocity is a scalar, $v_g = \partial\omega/\partial k$. However, the group velocity is parallel to the wavevector in band 1 whereas it is anti-parallel for band 2, and this is crucial to the operation of the proposed filter. The direction of propagation in the medium is defined by the frequency, and the matching of the components of the wavevector parallel to the interface, k_t , for the incident and refracted waves, and the requirement that v_g for the transmitted wave is propagating into the medium. In the case of a standard uniform isotropic medium, the EFS is a sphere, and matching of the component of the wavevector of an incident wave parallel to the interface leads to Snell's law and conventional positive refraction. Now consider a wave incident at angle α from a vacuum onto a PC, at a frequency which is within band 1 where the

EFS is near-isotropic and \mathbf{v}_g is essentially in the same direction as the wavevector. The respective magnitudes of the wavevectors in the vacuum and PC are k_{vacuum} and k_{PC} respectively and the angle of refraction is denoted by β . Therefore we have $k_{vacuum} \sin \alpha = k_{PC} \sin \beta = k_\tau$ as illustrated in Fig. 2(a). In this particular case, $f = 1.136$ THz and $\alpha = 20^\circ$. Since for this band \mathbf{v}_g is parallel to the wavevector positive refraction occurs. In

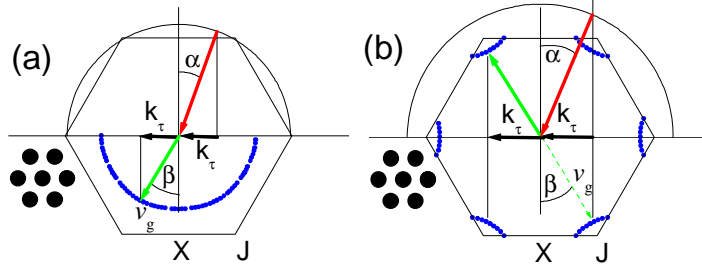


Fig. 2. The arrows indicate the wavevectors of the incident radiation (at angle α), the corresponding wavevectors in the photonic crystal (at angle β), and their component parallel to the interface (k_τ). The hexagon denotes the first Brillouin zone in the photonic crystal. (a) At frequency, $f = 1.136$ THz, within band 1 part of the near-isotropic equipfrequency surface (EFS) in the photonic crystal and the spherical EFS in the vacuum (upper half-space) are shown. The group velocity in the photonic crystal is in the same direction as the wavevector. In (b) in band 2 with $f = 1.344$ THz the EFS in the photonic crystal bandstructure is anisotropic and \mathbf{v}_g is in the direction of the dashed arrow, giving negative refraction.

contrast, at frequency $f = 1.344$ THz, which lies within band 2 with $f_J < f < f_X$, we find that the matching of k_τ together with the requirement that the transmitted wave is propagating away from the interface leads to the situation shown in Fig. 2(b). This corresponds to negative refraction. As a check on the calculations, we note that when the time-averaged Poynting vector is averaged over a unit cell of the structure, this gives a result in the same direction as the group velocity, as expected. The form of the bandstructure in Fig. 1 suggests that the onset of negative refraction should occur when $f = f_J = 1.28$ THz for which the transmitted wave and group velocity will be in a Γ -J direction with $\beta = 30^\circ$. As $k_\tau = (2\pi/a)/3$ at this point in the Brillouin zone, we can obtain α from the expression

$$k_\tau = k_{vacuum} \sin \alpha = k_{PC} \sin \beta \Rightarrow \sin \alpha = \frac{1}{3f_J} \left(\frac{c}{a} \right).$$

The minimum angle consistent with negative refraction via band 2 corresponds to $\alpha = 23^\circ$. At higher frequencies, as can be seen in the equipfrequency plot in Fig. 3, the EFS of band 2 becomes essentially circular. With fixed α and the magnitude of the wavevector reducing in the PC as the frequency increases, there is an upper cutoff frequency above which matching of k_τ can no longer be achieved at any angle, β , and hence negative refraction is suppressed. Using $\alpha = 23^\circ$ the cutoff frequency is 1.48 THz (at which point the tangential component of the wavevector has increased from 0.33 to 0.38 in units of $2\pi/a$), well below the band 2 maximum frequency of about 1.76 THz. As α is increased, the cutoff frequency is reduced. These results suggest that it should in principle be possible to channel the incident radiation into either positively or negatively refracted beams, depending on frequency, and further, that the width of the resultant pass-bands can, to some extent, be adjusted. When $\alpha = 23^\circ$ the bandstructure calculations suggest that positive refraction should be possible for frequencies

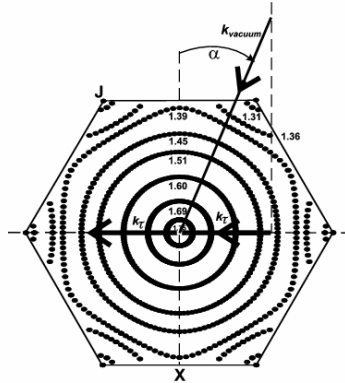


Fig. 3. Band 2 equipfrequency plot indicating the situation at cutoff.

1.08 - 1.28 THz, although, as with negative refraction, the value of the transmission coefficient also needs to be taken into account.

To investigate the above proposition concerning negative refraction and the effects of variation in transmission coefficient, we have carried out finite-difference time-domain simulations [9] involving plane waves at frequencies within both bands incident on a prism constructed from a hexagonal structure PC with a and d as above. Figure 4(a) shows a simulation of the intensity of the EM field pattern with $\alpha = 20^\circ$, $f = 1.136$ THz, in band 1. When incident on the "incident facet" (IF) the plane-wave experiences positive refraction,

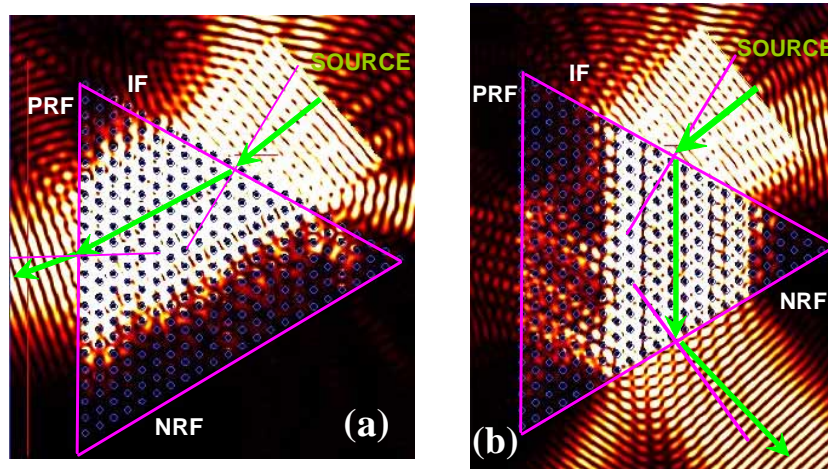


Fig. 4. Simulations of the electric field intensity when a plane-wave with $\alpha = 20^\circ$ is incident on the photonic crystal prism. The boundaries of the prism are highlighted. (a) For frequency $f = 1.136$ THz positive refraction occurs and light emerges from the PRF while in (b), with $f = 1.344$ THz the wave is negatively refracted and emerges from the NRF.

propagates through the prism and emerges from the "positive refraction facet" (PRF). In contrast, with $f = 1.344$ THz, which falls within band 2, we observe a rather different result, shown in Fig. 4(b). In this case negative refraction at both the IF and the "negative refraction facet" (NRF) is clearly visible. Note that there are some small artefacts due to internal reflection at the prism facets.

Figure 5 shows the spectral dependence of the radiation flux emerging from the PRF and NRF normalized to the flux of the incident beam when $\alpha = 20^\circ$. One can see from the emergent spectra from the PRF and NRF that the PC prism has given rise to separated transmission bands, which we will refer to as the PRF band and the NRF band respectively.

We also note that in the spectrum emergent from the NRF one can see small peaks overlapping with the position of the PRF band and vice versa, due to the aforementioned multiple internal reflection of the refracted beams within the prism, but that these are relatively small compared to the main transmission peaks.

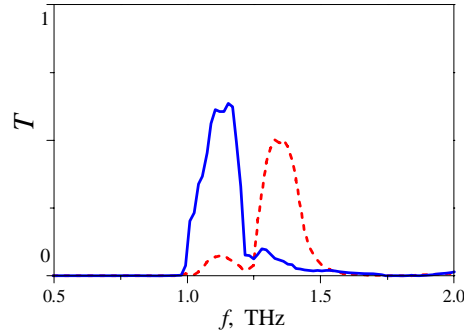


Fig. 5. Spectral dependence of the radiation flux emergent from the PRF (solid line) and the NRF (dashed line) normalized to the flux of the incident beam when $\alpha = 20^\circ$. The flux is calculated at the respective exit surfaces of the prism.

The features of the wave propagation through the PC prism suggest that such structures could be used as pass-band filters. In practice, the transmission spectrum is dependent upon the angle of incidence and the prism size and geometry, features which can be adjusted to provide an optimised transmission for a particular application. In Fig. 4(b) the angle and frequency have been chosen in order to maximise the transmission and the angle of deviation of the negatively refracted beam but significant transmission is observable over a range of incident angles from about $10 - 25^\circ$. Figure 6 shows the location of the PRF and NRF bands as a function of α . It can there be seen that the positions and widths of the transmission bands can be adjusted to some extent by varying α . The frequency of the PRF band increases and the frequency of the NRF band decreases with increasing angle. Outside the considered interval of angles, there is no well defined single pass-band, internal reflection in the prism increases and both PRF and NRF beam intensities become comparable. In this figure the band width and therefore the gap between the bands, has been defined via the half-width of the respective bands. Consequently, we cannot directly compare the positions of the edges with those of the bandstructure calculations, which are defined via the absolute edges of the respective bands. However, we note that the mid-point between the PRF and NRF bands suggests that $f_j = 1.25$ THz, in good agreement with the bandstructure results.

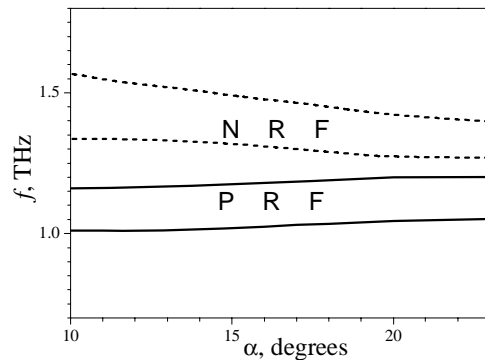


Fig. 6. Solid lines show the boundaries of the PRF band as a function of α , while dashed lines show the boundaries of the NRF band.

3. Conclusions

We have theoretically demonstrated a terahertz pass-band filter with separate pass-bands based on a metallic photonic crystal prism by utilizing the distinction between positive and negative refraction. Photonic bandstructure calculations have been used to explain the basic principles of operation of the prism and finite-difference time-domain simulations have been employed to provide the detailed predictions concerning the nature of the transmission in the structure considered. It has been demonstrated that by varying the angle of incidence, it is possible to tune the positions and widths of the pass-bands to a limited extent.

Acknowledgment

The work was funded by EPSRC, UK, via grant no. EP/C534263.